CHEMISTRY OF MATERIALS
Article

Chem. Mater. **2009,** *21,* 3325–3331 3325
DOI:10.1021/cm900841t

Ferromagnetism and Magnetocaloric Effect around 95 K in the Laves Phase $EuRh_{1.2}Zn_{0.8}$

Wilfried Hermes, Thomas Harmening, and Rainer Pöttgen*

Institut für Anorganische und Analytische Chemie and NRW Graduate School of Chemistry, Universität Münster, Corrensstrasse 30, D-48149 Münster, Germany

Received March 26, 2009. Revised Manuscript Received May 22, 2009

Samples of the solid solution $EuRh_{2-x}Zn_x$ with $x \approx 1$ were synthesized by high-frequency melting of the elements in sealed tantalum tubes. They crystallize with the structure of the cubic Laves phase $MgCu_2$. The structure of one crystal was refined from single-crystal X-ray diffractometer data: space group $Fd\bar{3}m$, $a = 768.58(6)$ pm, $wR_2 = 0.0121$, 99 F^2 values, 6 variables. The rhodium and zinc atoms statistically occupy the 16*d* site of the three-dimensional tetrahedral network. The europium atoms have coordination number 16 by 12 Rh/Zn and 4 Eu neighbors. The sample with nominal composition $EuRh_{1.2}Zn_{0.8}$ was studied with respect to its physical properties. $EuRh_{1.2}Zn_{0.8}$ shows stable divalent europium (8.00 μ_B/Eu atom) and orders ferromagnetically at $T_C = 95$ K. Magnetization isotherms characterize $EuRh_{1.2}Zn_{0.8}$ as a soft ferromagnet. ^{151}Eu Mössbauer spectroscopic data confirm the europium valence state ($\delta = -7.44$ mm/s at 77 K) and the magnetic ordering. According to magnetocaloric investigations, $EuRh_{1.2}Zn_{0.8}$ has a quite high normalized relative cooling power with 103 J $K^{-1}T^{-1}$ for $\Delta H = 5$ T, which makes it an interesting cooling material.

1. Introduction

The binary europium-based Laves phases EuX_2 (X = Rh,[1−4] Ir,[5,6] Pd,[7,8] Pt,[8,9] and Al[10,11]) have been intensively studied with respect to their interesting physical properties. Depending on the X component, europium is trivalent or divalent, connected with magnetic ordering at comparatively high ordering temperatures. An interesting task is the study of potential valence changes of europium, associated with changes in the physical properties. Such variations can be achieved by partial substitution of the X component by another element, by application of temperature and/or high pressure, or via hydrogenation. A highly interesting example in that view is the hydride $EuRh_2H_x$.[3] Buschow et al. have shown that hydrogenation of $EuRh_2$ leads to the hydride $EuRh_2H_x$, and the europium valence switches from +III to +II.

In the present work, we use another approach for tuning the europium valence. The reduction of the trivalent Eu-atoms in $EuRh_2$ is achieved by substituting rhodium by the more electropositive zinc within a solid solution $EuRh_{2-x}Zn_x$ with $x \approx 1$. For the trivalent rare earth elements (except Ce, which behaves almost tetravalent[12]) the whole RERhZn series has recently been reported.[12,13] The RERhZn compounds with RE = La, Ce, Pr, Nd crystallize with the orthorhombic LaNiAl type, whereas those with the smaller rare earth elements adopt the TiNiSi structure. In the latter series, the europium member was missing. Keeping these results in mind, we synthesized $EuRh_{1.2}Zn_{0.8}$. This intermetallic zinc compound, however, adopts the structure of the cubic Laves phase $MgCu_2$ with a random occupation of rhodium and zinc on the tetrahedral copper network. The structure−property relationships of this new compound are reported herein. The focus on the present investigation lies on the magnetic properties and the magnetocaloric effect (MCE). Because Eu^{2+} has seven unpaired f-electrons like Gd^{3+}, it is also an attractive element for MCE materials. Unfortunately, intermetallic europium-based compounds are mostly showing low-ordering temperatures and therefore have only scarcely been investigated with respect to MCE. One example for a detailed study of the MCE of europium-containing compounds is

*Corresponding author. Fax: 49 251 83 36002. E-mail: pottgen@uni-muenster.de.

(1) Wickman, H. H.; Wernick, J. H.; Sherwood, R. C.; Wagner, C. F. *J. Phys. Chem. Solids* **1968**, 29, 181.
(2) Bauminger, E. R.; Felner, I.; Levron, D.; Nowik, I.; Ofer, S. *Solid State Commun.* **1976**, 18, 1073.
(3) Buschow, K. H. J.; Cohen, R. L.; West, K. W. *J. Appl. Phys.* **1977**, 48, 5289.
(4) Iandelli, A.; Palenzona, A. *Rev. Chim. Minér.* **1983**, 20, 449.
(5) Pöttgen, R.; Hoffmann, R.-D.; Möller, M. H.; Kotzyba, G.; Künnen, B.; Rosenhahn, C.; Mosel, B. D. *J. Solid State Chem.* **1999**, 145, 174.
(6) De Vries, J. W. C.; Thiel, R. C.; Buschow, K. H. J. *Physica B* **1984**, 124, 291.
(7) Iandelli, A.; Palenzona, A. *J. Less-Common Met.* **1974**, 38, 1.
(8) Kropp, H.; Zipf, W.; Dormann, E.; Buschow, K. H. J. *J. Magn. Magn. Mater.* **1979**, 13, 224.
(9) Erdmann, B.; Keller, C. *J. Solid State Chem.* **1973**, 7, 40.
(10) Harris, I. R.; Mansey, R. C.; Raynor, G. V. *J. Less-Common Met.* **1965**, 9, 270.
(11) Mader, K. H.; Wallace, W. E. *J. Chem. Phys.* **1968**, 49, 1521.
(12) Hermes, W.; Al Alam, A. F.; Matar, S. F.; Pöttgen, R. *Solid State Sci.* **2008**, 10, 1895.
(13) Hermes, W.; Pöttgen, R. *Solid State Sci.* **2009**, 11, 706.

Published on Web 06/18/2009

the clathrate $Eu_8Ga_{16}Ge_{30}$, with a low-temperature giant MCE.[14]

The europium valence can easily be monitored by ^{151}Eu Mössbauer spectroscopy which reveals well separated signals for divalent (around −10 mm/s) and trivalent (around 0 mm/s) europium. In the large family of EuTX compounds with divalent europium, the isomer shift δ depends on the number of valence electrons per formula unit. δ decreases from ca. −8 mm/s for 14 VE/fu to ca. −11 mm/s for 18 VE/fu.[15,16] The so far lowest number of 14 VE/fu was observed for EuRhIn.[16] As reported herein, further reduction of the valence electron concentration is possible via indium substitution by zinc.

2. Experimental Section

Synthesis. Starting materials for the preparation of the $EuRh_{2-x}Zn_x$ (x = 0.5−1.5) samples were ingots of europium (Johnson Matthey), rhodium powder (Degussa-Hüls, 200 mesh), and zink granules (Merck), all with stated purities better than 99.9%. The air- and moisture sensitive europium ingots were kept in Schlenk tubes under dry argon prior to the reaction. Argon was purified with titanium sponge (900 K), silica gel, and molecular sieves. The elements were weighed in the ideal atomic ratio and sealed in a tantalum ampule under an argon pressure of 800 mbar in an arc-melting apparatus.[17] The tantalum ampule was subsequently placed in the water-cooled sample chamber of an induction furnace[18] (Hüttinger Elektronik, Freiburg, Germany, Typ TIG 2.5/300), heated to 1500 K, and kept at that temperature for 10 min. Finally, the temperature was lowered to 900 K, and the sample was annealed at that temperature for another 5 h and then cooled within the furnace after the power was switched off. The temperature was controlled by a Sensor Therm Methis MS09 pyrometer with an accuracy of ±30 K. No reaction with the container material was observed. The compact light-gray pieces and the dark-gray powder were stable in air.

EDX Analyses. All bulk samples and the single crystals of $EuRh_{2-x}Zn_x$ (x = 0.5−1.5) investigated on the diffractometers were semiquantitatively analyzed by EDX using a Leica 420i scanning electron microscope with EuF_3, rhodium, and zinc as standards. The single crystals glued on quartz fibers were coated with a thin carbon film to enable electrical conductivity. The polycrystalline bulk samples were embedded in a methylmetacrylate matrix. They were polished with diamond and SiO_2 emulsions with different grain sizes. The experimentally observed phases in bulk samples with zinc rich starting compositions $EuRh_{2-x}Zn_x$ with $x > 1$ were $EuRh_{1.1}Zn_{0.9}$, EuZn, and $EuZn_2$. Starting compositions with x varying from 0.7 to 0.9 yielded single-phase compounds with a homogeneity range of $x \approx 0.7-0.9$, whereas $x < 0.7$ revealed $EuRh_{2-x}Zn_x$ (x = 0.7−0.9) and the binary $EuRh_2$. No impurity elements heavier than sodium (detection limit of the instrument) were found. We observe similar results from X-ray powder diffraction. These observations imply that the solid solution $EuRh_{2-x}Zn_x$ exists up to $x \approx 1$. With lower zinc contents, however, there are preparation difficulties most likely due to the high difference between the melting points of rhodium and zinc. With higher rhodium contents, higher reaction and annealing temperatures are necessary, but then zinc starts to evaporate. This results in multiphase samples. High-pressure, high-temperature preparation techniques might be helpful for synthesis of the zinc-poorer samples.

Table 1. Crystal Data and Structure Refinement for $EuRh_{1.08(2)}Zn_{0.92(2)}$

empirical formula	$EuRh_{1.08(2)}Zn_{0.92(2)}$
structure type	$MgCu_2$
space group; Z	$Fd\bar{3}m$; 8
molar mass, g/mol	323.15
unit-cell dimensions (crystal) (pm)	768.58(6)
Guinier powder data (pm)	770.2(2)
V (nm^3)	V = 0.4540
ρ (g/cm^3)	9.46
crystal size (μm^3)	20 × 40 × 60
transmission ratio (max/min)	0.648/0.551
radiation	Ag K$_\alpha$ (λ = 56.083 pm)
μ (mm^{-1})	23.4
F(000)	1113
θ range (deg)	3−32
range in hkl	±12, ±12, ±14
total no. of reflections	1808
independent reflections	99 (R_{int} = 0.0252)
reflections with $I \geq 2\sigma(I)$	82 (R_{sigma} = 0.0430)
data/parameters	99/6
GOF on F^2	1.207
final R indices [$I \geq 2\sigma(I)$]	R_1 = 0.0095 wR_2 = 0.0114
R indices (all data)	R_1 = 0.0168 wR_2 = 0.0121
extinction coeff	0.00138(9)

X-ray Powder Diffraction and Single-Crystal Data Collection. The polycrystalline samples $EuRh_{2-x}Zn_x$ (x = 0.5−1.5) were characterized by Guinier patterns (imaging plate detector, Fujifilm BAS-1800) with Cu$K\alpha_1$ radiation and α-quartz (a = 491.30, c = 540.46 pm) as an internal standard. All samples were composed of a nearly 1:1:1 phase with similar lattice parameters and the side products described before (EDX analyses, *vide ultra*). For starting compositions of $EuRh_{2-x}Zn_x$ (x = 0.7−0.9) Guinier powder patterns showed phase-pure samples that crystallize with the structure of the cubic Laves phase $MgCu_2$. The cubic lattice parameter (Table 1) was deduced from least-squares refinements. Small irregularly shaped single crystals of refined compositions (vide infra) $EuRh_{1.08(2)}Zn_{0.91(2)}$ and $EuRh_{1.11(6)}Zn_{0.89(6)}$ were selected from the crushed samples of the nominal compositions $EuRh_{1.2}Zn_{0.8}$ and $EuRh_{1.0}Zn_{1.0}$. They were tested by Laue photographs on a Buerger camera using white Mo radiation. Intensity data were then collected at room temperature by use of a four-circle diffractometer (CAD4) with graphite monochromatized Ag Kα radiation and a scintillation counter with pulse height discrimination. The scans were taken in the $\omega/2\theta$ mode and empirical absorption corrections were applied on the basis of psi-scan data, accompanied by spherical absorption corrections. Because of the similar compositions of the two crystals, we present only all relevant details concerning the data collections and evaluations of one of them in Table 1.

Physical Property Measurements and Mössbauer Spectroscopy. The single phase $EuRh_{1.2}Zn_{0.8}$ sample was packed in kapton foil and attached to the sample holder rod of a VSM for measuring the magnetic properties in a Quantum Design Physical-Property-Measurement-System in the temperature range 3.1−305 K with magnetic flux densities up to 80 kOe.

(14) (a) Phan, M. H.; Woods, G. T.; Chaturvedi, A.; Stefanoski, S.; Nolas, G. S.; Srikanth, H. *Appl. Phys. Lett.* **2008**, 93, 252505.(b) Bentien, A.; Paschen, S.; Pacheco, V.; Grin, Yu.; Steglich, F. Proceedings of the 22nd International Conference on Thermoelectrics; IEEE: Piscataway, NJ, 2003; p 131
(15) Müllmann, R.; Mosel, B. D.; Eckert, H.; Kotzyba, G.; Pöttgen, R. *J. Solid State Chem.* **1998**, 137, 174.
(16) Müllmann, R.; Ernet, U.; Mosel, B. D.; Eckert, H.; Kremer, R. K.; Hoffmann, R.-D.; Pöttgen, R. *J. Mater. Chem.* **2001**, 11, 1133.
(17) Pöttgen, R.; Gulden, Th.; Simon, A. *G.I.T. Lab. J.* **1999**, 43, 133.
(18) Kuβmann, D.; Hoffmann, R.-D.; Pöttgen, R. *Z. Anorg. Allg. Chem.* **1998**, 624, 1727.

For heat capacity (C_P) measurements (3−300 K, $H = 0$, 10, and 30 kOe) the sample was glued to the platform of a precalibrated heat capacity puck using Apiezon N grease.

The 21.53 keV transition of ^{151}Eu with an activity of 130 MBq (2% of the total activity of a ^{151}Sm:EuF_3 source) was used for the ^{151}Eu Mössbauer spectroscopic experiments. The measurements were performed in the usual transmission geometry in commercial helium bath and flow cryostats. The temperature of the absorber could be varied from 4.2 to 300 K. The source was kept at room temperature in all experiments. The sample was placed within a thin-walled PVC container at a thickness corresponding to about 10 mg Eu/cm^2.

3. Results and Discussion

Structure Refinement. The diffractometer data set was compatible with space group $Fd\bar{3}m$, similar to $EuRh_2$.[1−4] Consequently, as starting model, the europium atoms were placed on the 8*a* site and on the 16*d* site we introduced a mixed occupancy of Rh/Zn. The structure was then refined using SHELXL-97[19] (full-matrix least-squares on F^2) with anisotropic atomic displacement parameters for all atoms, and the Rh/Zn ratio was refined as a least-squares variable. The final difference Fourier synthesis was flat (Table 1). The atomic parameters and interatomic distances are listed in Tables 2 and 3. Further details on the structure refinement are available.[20]

Refinement in space group $Fd\bar{3}m$ does not allow a 1:1 ordering of rhodium and zinc within the tetrahedral network. Also, in the maximal subgroups, this kind of ordering is not possible. The composition of the crystal selected from the sample of the nominal composition $EuRh_{1.2}Zn_{0.8}$ was refined to $EuRh_{1.08(2)}Zn_{0.92(2)}$. It is clear that a distribution of compositions $EuRh_{1+x}Zn_{1-x}$ exists in this sample. For the property investigations (vide infra), the phase-pure sample of the nominal composition $EuRh_{1.2}Zn_{0.8}$ was used.

The isotropic displacement parameter of the europium atoms is slightly larger than the one of the mixed occupied site. Refinement of the occupancy parameters revealed full occupancy of the europium site. Probably the displacement parameter is indicative of weak rattling of the europium atoms within the coordination number 16 cage.

Crystal Chemistry. The intermetallic zinc compound $EuRh_{1.08}Zn_{0.92}$ crystallizes with the structure of the cubic Laves phase $MgCu_2$, space group $Fd\bar{3}m$, similar to $EuRh_2$.[1−4] The rhodium and zinc atoms show statistical distribution on the three-dimensional network of corner-sharing $Cu_{4/4}$ tetrahedra (Figure 1). In binary $EuRh_2$, the rhodium atoms within the tetrahedral network are at 266 pm Rh−Rh, slightly shorter than in fcc rhodium.[21] Each europium atom has coordination number 16, i.e., 12 × Eu−Rh at 312 pm and 4 × Eu−Eu at 326 pm in the form of a Frank−Kaspar polyhedron.[22,23] The rhodium−zinc substitution leads to a significant unit-cell enlargement from $a = 752$ pm for $EuRh_2$ to $a = 770$ pm for $EuRh_{1.2}Zn_{0.8}$ and thus to an overall increase in the interatomic distances.

The increase in the unit cell through the rhodium−zinc substitution is surprising, because rhodium and zinc both have a covalent radius[24] of 125 pm; therefore, it is attributed to electronic reasons because of the change from trivalent to divalent europium (vide infra). Also, the Rh(Zn)−Rh(Zn) distances of 272 pm are significantly longer than the sum of the covalent radii of 250 pm. However, they compare well with the Rh−Zn distances observed in the LaNiAl or TiNiSi type RERhZn compounds, e.g., 263−284 pm in CeRhZn.[12]

The formation of a cubic or hexagonal Laves phase depends on the number of valence electrons (VE) per formula unit (fu). Johnston and Hoffmann have

Table 2. Atomic Coordinates and Anisotropic Displacement Parameters (pm^2) of $EuRh_{1.08(2)}Zn_{0.92(2)}$[a]

Atom	Wyckoff position	Occupancy %	*x*	*y*	*z*	U_{11}	U_{12}
Eu	8*a*	100	1/8	1/8	1/8	150(1)	0
Rh	16*d*	54(1)	1/2	1/2	1/2	136(1)	−5(1)
Zn	16*d*	46(1)	1/2	1/2	1/2	136(1)	−5(1)

[a] U_{eq} is defined as one third of the trace of the orthogonalized U_{ij} tensor. The anisotropic displacement factor exponent takes the form $-2\pi^2[(ha^*)^2U_{11} + \ldots + 2hka^*b^*U_{12}]$. $U_{11} = U_{22} = U_{33} = U_{eq}$. $U_{12} = U_{23} = U_{13}$.

Table 3. Interatomic Distances (pm), Calculated with the Crystal Lattice Parameter of $EuRh_{1.08(2)}Zn_{0.92(2)}$[a]

Eu:	12	Rh/Zn	318.6	Rh/Zn:	6	Rh/Zn	271.7
	4	Eu	332.8		6	Eu	318.6

[a] Standard deviations are all less than 0.1 pm. All distances within the first coordination spheres are listed.

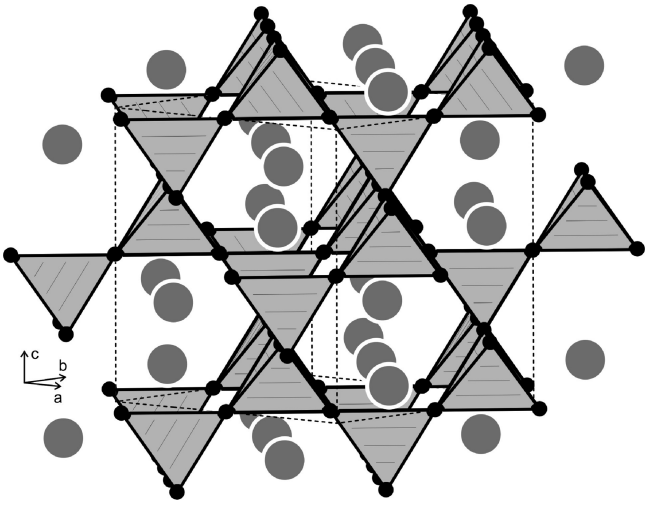

Figure 1. Crystal structure of $EuRh_2$. Europium and rhodium atoms are drawn as medium gray and black circles, respectively. The three-dimensional network of corner-sharing $Rh_{4/4}$ tetrahedra is emphasized.

(19) Sheldrick, G. M. Shelxl-97, Program for Crystal Structure Refinement; University of Göttingen: Göttingen, Germany, 1997.
(20) Further details on the structure refinement are available from Fachinformationszentrum Karlsruhe, D-76344 Eggenstein-Leopoldshafen, Germany, by quoting the Registry No. CSD−420538.
(21) Donohue, J. The Structures of the Elements; Wiley: New York, 1974.
(22) Frank, F. C.; Kaspar, J. S. *Acta Crystallogr.* **1958**, 11, 184.
(23) Frank, F. C.; Kaspar, J. S. *Acta Crystallogr.* **1959**, 12, 483.
(24) Emsley, J. The Elements; Clarendon Press: Oxford, U.K., 1989.

calculated the stability ranges on model AB_2 compounds.[25] In the range from 20 to 25 electrons per formula unit, the cubic phase is the stable one. This is in fact realized for $EuRh_2$ (trivalent europium) with 21 and $EuRh_{1.2}Zn_{0.8}$ (divalent europium, vide infra) with around 22−23 VE/fu. For a more detailed discussion on the crystal chemistry and chemical bonding in such Laves phases, we refer to recent review articles.[25−29]

As already mentioned in the introduction, six binary europium based Laves phases are known EuX_2 (X = Rh,[1−4] Ir,[5,6] Pd,[7,8] Pt,[8,9] and Al[10,11]) and the isotypic hydride $EuRh_2H_x$.[3] If we compare the Eu−Eu distances and relate them to the magnetic properties, we can see that for the shortest distances from 326 to 328 pm, the europium atoms are in a trivalent state.[3,6] For the longest distances of 352 (X = Al) and 361 pm (X = RhH_x), the europium atoms are divalent and order at Néel temperatures of $T_{N1} = 30$ and $T_{N2} = 15$ K (X = Al)[11] and 15.5 K (X = RhH_x).[3] Within the moderate distances of 336 (X = Pd), 334 (X = Pt), and 333 pm (X = Rh/Zn), the Eu atoms are in a divalent state too, but order ferromagnetically at Curie temperatures of 80,[8] 105,[8] and around 95 K, respectively. These ordering temperatures are quite high when compared with other intermetallic europium compounds. Hence, the magnetic ordering and the temperatures seem to be dominated by the interatomic Eu−Eu distances and not predominantly by the nature of the X element in these binary and pseudobinary Laves phases.

Magnetic Properties. Figure 2 shows the temperature dependence of the susceptibility ($\chi = M/H$) and the inverse susceptibility χ^{-1} with an external applied field of 10 kOe. The curve reveals the ferromagnetic nature of the compound around the Curie temperature (T_C) of 95 K. The effective paramagnetic moment was calculated in the paramagnetic region. The values obtained are μ_{eff} = 8.00(1) μ_B/Eu atom and θ = 103(1) K, as compared with the respective free ion value of 7.94 μ_B for Eu^{2+}. Such a large positive value of θ agrees with the ferromagnetic character of $EuRh_{1.2}Zn_{0.8}$.

The ZFC-FC measurement with an applied field of 100 Oe is plotted in Figure 3. The Curie temperature is corresponding to the peak of the derivative of the susceptibility ($d\chi/dT$) (see the inset of Figure 2). The relatively broad ordering temperature even at a low field of 100 Oe is due to several domains with slightly different compositions in this sample, but can not be avoided by synthesis. The domains also slightly inhibit the long-range ordering of the Eu moments. If the long-range ordering is not completely outspreaded, the dc−$\chi(T)$ will show a field dependency and bifurcation of the ZFC-FC curves. This is well-known from the spin- (or cluster-) glass-systems, where the long-range ordering is absent. The $\chi(T)$ values

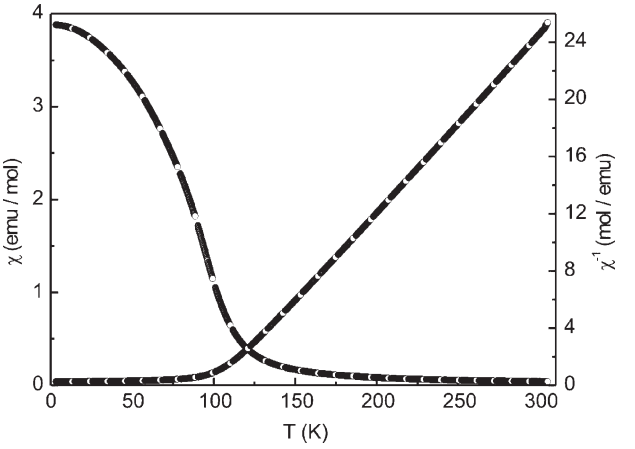

Figure 2. Susceptibility χ and inverse susceptibility χ^{-1} for $EuRh_{1.2}Zn_{0.8}$ in H = 10 kOe.

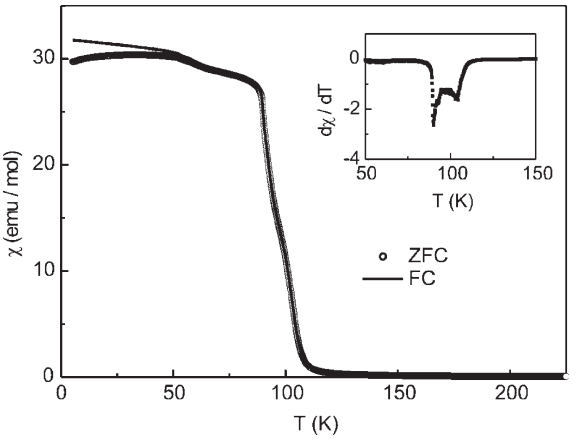

Figure 3. Low-temperature susceptibility (zero-field-cooling and field-cooling modus) of $EuRh_{1.2}Zn_{0.8}$ at 100 Oe (kink-point measurement). The inset shows the derivative $d\chi/dT$ of the zero-field-cooling curve with a broad peak at the Curie temperature. For details, see text.

of the low-field measurement below the ordering temperature (the maximum is approximately 30 emu/mol) decrease with increasing field strengths (approximately 4 emu/mol at 10 kOe) and the ZFC-FC curve splits somewhat at around 50 K, indicating a slight suppression of the long-range ordering in line with all other measurements (vide infra and ultra). In comparison with $EuRh_2H_x$ (magnetic ordering temperature T_O = 15.5 K),[3] the Curie temperature of the $EuRh_{1.2}Zn_{0.8}$ sample is significantly higher.

Several Laves phases REX_2 (RE = rare earth or yttrium, X = transition metal) have attracted considerable attention in recent years due to their intrinsic magnetic structures and transport properties as well as potential applications to magnetic refrigeration technology.[30−34] Because

(25) Johnston, R. L.; Hoffmann, R. *Z. Anorg. Allg. Chem.* **1992**, 616, 105.
(26) Simon, A. *Angew. Chem.* **1983**, 95, 94.
(27) Nesper, R. *Angew. Chem.* **1991**, 103, 805.
(28) Nesper, R.; Miller, G. J. *J. Alloys Compd.* **1993**, 197, 109.
(29) Gschneidner, K. A.Jr; Pecharsky, V. K. *Z. Kristallogr.* **2006**, 221, 375.
(30) Singh, N. K.; Suresh, K. G.; Nigam, A. K.; Malik, S. K.; Coelho, A. A.; Gama, S. *J. Magn. Magn. Mater.* **2007**, 317, 68.
(31) von Ranke, P. J.; Grangeia, D. F.; Caldas, A.; de Oliveira, N. A. *J. Appl. Phys.* **2003**, 93, 4055.
(32) Herrero-Albillo, J.; Bartolomé, F.; García, L. M.; Casanova, F.; Labarta, A.; Batlle, X. *Phys. Rev. B* **2006**, 73, 134410.
(33) Wang, F. W.; Zhang, X. X.; Hu, F. X. *Appl. Phys. Lett.* **2000**, 77, 1360.
(34) Gschneidner, K. A. ; Pecharsky, V. K.; Tsokol', A. O. *Rep. Prog. Phys.* **2005**, 68, 1479.

$EuRh_{1.2}Zn_{0.8}$ exhibits a second-order magnetic transition (SOMT) and crystallizes with the structure of the cubic Laves phase $MgCu_2$, we have also determined the magnetocaloric behavior.

As shown in Figure 4, $EuRh_{1.2}Zn_{0.8}$ behaves as a soft ferromagnet with negligible remanence. No magnetic hysteresis loss is observed. Isothermal magnetization performed at low temperatures, for example at 5 K, saturates already at 2 T with 7.12 μ_B per Eu atom, only slightly higher than the theoretically calculated free Eu^{2+} ion value ($g \times J = 7\ \mu_B$).

Figure 5 shows the so-called Arrott's plot (converted M (H) isotherms into M^2 vs. H/M). According to the Banerjee criterion[35] the magnetic transition is of second order if all the H/M versus M^2 curves have positive slope. On the other hand, if some of the H/M versus M^2 curves show negative slope at some point, the transition is of first order.[35,36] For the case of $EuRh_{1.2}Zn_{0.8}$, the presence of the positive slope of the H/M versus M^2 curves indicates that the magnetic transition is of second order. At around 100 K M^2 vs H/M runs almost like a straight line through the origin, indicating the vicinity to the ordering temperature. The MCE is characterized by the isothermal magnetic entropy change. By using the Maxwell relation $(\partial S/\partial H)_T = (\partial M/\partial T)_H$, the magnetic entropy change can be represented as

$$\Delta S_M = \int_0^H (dM/dT)_H \, dH$$

This expression shows that the sign of ΔS_M is determined by the sign of $(\partial M/\partial T)_H$. The sign of ΔS_M in $EuRh_{1.2}Zn_{0.8}$ is negative, showing conventional cooling by adiabatic demagnetization. From the magnetic isotherms (Figure 6) of $EuRh_{1.2}Zn_{0.8}$, we have derived values of ΔS_M as a function of temperature (see Figure 7). The relative cooling power (RCP) is a measure of how much heat can be transferred between cold and hot sinks in one ideal refrigerant cycle,[37] which is of practical significance. RCP is given by $RCP = -\Delta S_{maxM} \delta T_{fwhm}$.[38] ΔS_M reaches at the peak maximum −3.1 and −5.7 J kg^{-1} K^{-1}, δT_{fwhm} is 75 and 90 K, and the resulting RCP = 233 and 513 J kg^{-1}, for a field change of 2 and 5 T, respectively.

Because of the domains with slightly different compositions in the $EuRh_{1.2}Zn_{0.8}$ sample, ΔT_{pt} (temperature shift of the phase transition) is difficult to determine, a rough estimation gives 15−20 K. Indirect determination of ΔT_{ad} can be performed from the measured magnetization and temperature dependence of the heat capacity.[39]

$$\Delta T_{ad} = -T[S_{M,H\neq 0}(T) - S_{M,H=0}(T)]/C_0(T)$$

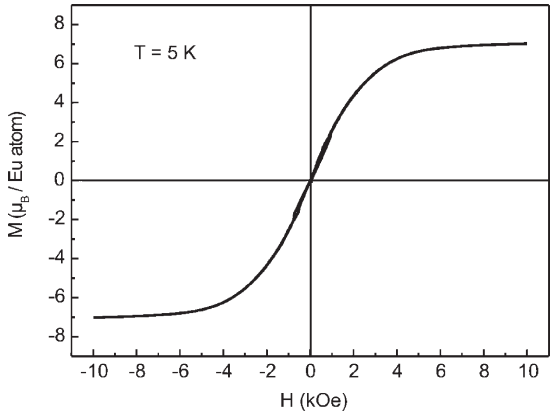

Figure 4. Hysteresis loop of $EuRh_{1.2}Zn_{0.8}$ measured at $T = 5$ K.

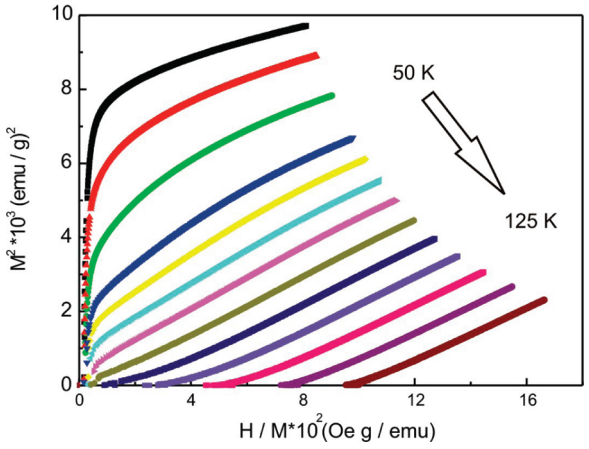

Figure 5. Arrott plots of $EuRh_{1.2}Zn_{0.8}$ from 50 to 125 K with different temperature steps.

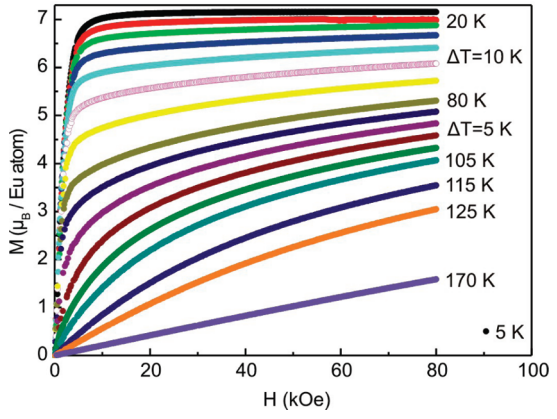

Figure 6. Magnetization isotherms of $EuRh_{1.2}Zn_{0.8}$ measured at various temperatures.

The temperature dependence of the heat capacity at zero field, $C_o(T)$, and at fields of 1 and 3 Tesla are shown in Figure 8. In the zero field measurement, the λ-like peak (though not very sharp) has broadness (ΔT) of 26 K (from the C_P maximum of 87 K to the minimum at 113 K). This broadness is due to the domains having slightly different compositions in $EuRh_{1.2}Zn_{0.8}$. This behavior did not change for annealed samples. The transition in $EuRh_{1.2}Zn_{0.8}$ is also broader than in fully hydrogenated

(35) Banerjee, S. K. *Phys. Lett.* **1964**, 12, 16.
(36) Mira, J.; Rivas, J.; Rivadulla, F.; Vázquez-Vázquez, C.; López-Quintela, M. A. *Phys. Rev. B* **1999**, 60, 2998.
(37) Giauque, W. F.; MacDougall, D. P. *Phys. Rev.* **1933**, 43, 768.
(38) Gschneidner, K. A.Jr.; Pecharsky, V. K. *Annu. Rev. Mater. Sci.* **2000**, 30, 387.
(39) Pecharsky, V. K.; Gschneidner, K. A.Jr. *J. Appl. Phys.* **1999**, 86, 565.

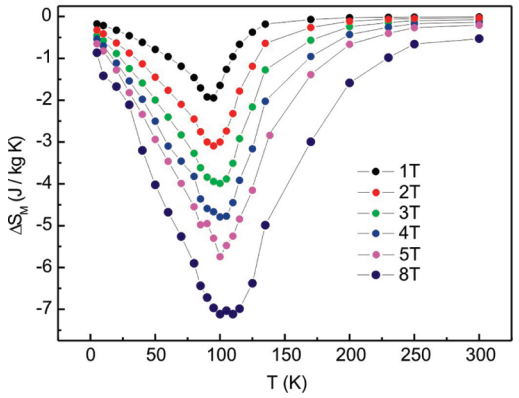

Figure 7. Temperature dependence of the magnetic-entropy change ΔS_M of $EuRh_{1.2}Zn_{0.8}$ for magnetic-field changes $\Delta H = 0-8$ T.

Table 4. Fitting Parameters for ^{151}Eu Mössbauer Spectroscopic Measurements on the $EuRh_{1.2}Zn_{0.8}$: Isomer Shift (δ), Electric Quadrupole Interaction (ΔEQ), Experimental Line Width (Γ), Average Magnetic Hyperfine Field ($\langle B_{eff}\rangle$), and Gaussian Standard Deviation of B_{eff} (σ_B)

T (K)	δ (mm/s)	Γ (mm/s)	ΔE_Q (mm/s)	$\langle B_{eff}\rangle$ (T)	σ_B (T)
298	−7.36(2)	2.58(6)	5.3(2)		
78	−7.44(2)	3.1(1)	−0.5(2)	4.80(7)	
4.2	−6.93(3)	2.5[a]	−1.0(2)	12.19(9)	3.30(9)

[a] Fixed parameter

$EuRh_2H_x$,[3] indicating that the hydride has smaller distribution of domains. The application of a field with strength of 1 T diminishes the cusp and with an applied field of 3 T the cusp gets broader. A shift of the transition temperature to higher temperatures is clearly visible. $C_o(T)$ shows a value of 205 J kg^{-1}K^{-1} at the peak entropy change, which results in $\Delta T_{ad} \approx 1.4$ and 2.8 K for $\Delta H = 2$ and 5 T, respectively.

^{151}Eu Mössbauer Spectroscopy. The ^{151}Eu Mössbauer spectra of $EuRh_{1.2}Zn_{0.8}$ at 4.2, 78, and 298 K are presented in Figure 9 with the fitting parameters listed in Table 4. The spectra are showing one major signal at −7.36(2) mm/s (at 298 K) and a minor component in the vicinity of 1 mm/s having ~10% of the overall intensity, attributed to a Eu^{3+} contribution, most likely resulting from surface oxidation of the polycrystalline sample, as has also been observed for other EuTX compounds.[5,15,16] This Eu^{III} signal is included as a broad Lorentzian in the fit at all temperatures. The spectra reveal significant quadrupole interactions, which are created by breaking the local cubic europium site symmetry, because of the mixed occupancy on the Rh/Zn site. The almost temperature independent isomer shift value suggests the europium atoms to be in a stable divalent state, as is already evident from magnetic susceptibility measurements (vide ultra). However, it is a remarkably low negative value, indicating a substantial s-electron density. Regarding the low valence electron count (VEC) of ~13 (assuming two electrons contributed from zinc), the isomer shift value agrees well with the correlation previously found for equiatomic EuTX compounds.[16] The extended correlation plot is shown in the inset of Figure 9.

At 4.2 K, and therefore clearly below T_C, magnetic hyperfine splitting is observed. A proper fit can only be

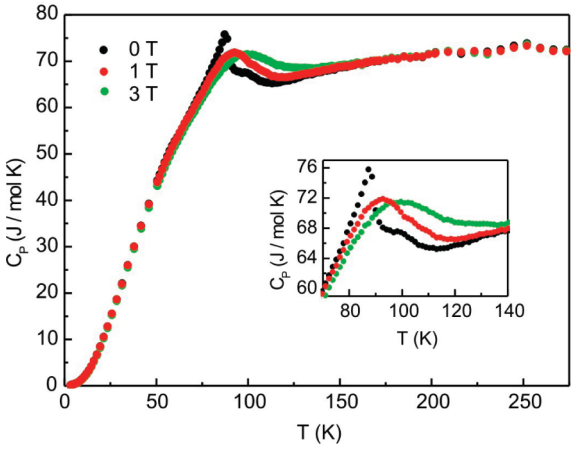

Figure 8. Temperature dependence of the specific heat of $EuRh_{1.2}Zn_{0.8}$ in externally applied field strengths of 0, 1, and 3 T. The behavior around the Curie temperature is highlighted in the inset.

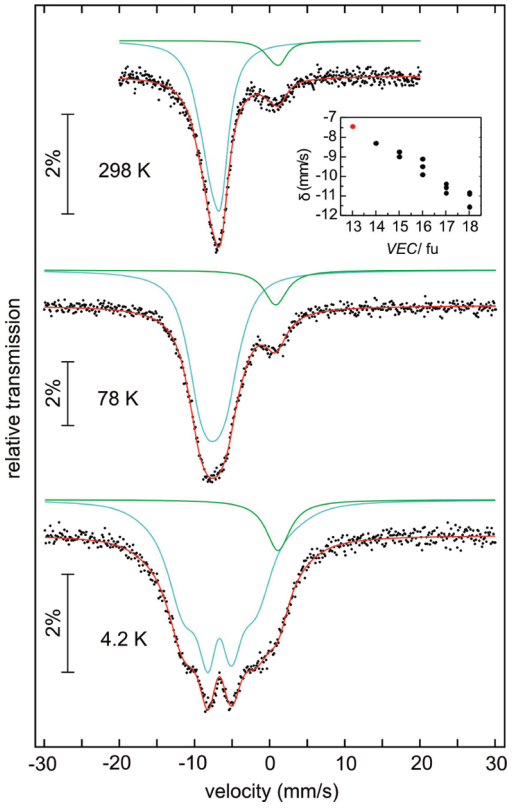

Figure 9. Experimental and simulated ^{151}Eu Mössbauer spectra of $EuRh_{1.2}Zn_{0.8}$. The inset shows the correlation plot of the ^{151}Eu Mössbauer isomer shifts (at 78 K) versus the valence electron count (VEC) per formula unit for various ternary EuTX intermetallics reproduced from ref 15 (for details see text). The red point presents $EuRh_{1.2}Zn_{0.8}$. For details, see text.

obtained by assuming a Gaussian distribution of magnetic hyperfine field strengths with a standard deviation of 3.30(9) T. A reasonable explanation is the occurrence of a local field distribution due to multiple local environments [$EuRh_{12-x}Zn_x$ ($x \approx 6$)]. Furthermore, the absolute value of the magnetic flux density is rather small, compared to those observed in related compounds.[15,16] In terms of the relatively high s-electron density observed for $EuRh_{1.2}Zn_{0.8}$, this is in agreement with the relation

between hyperfine field and isomer shift, as suggested by Wickman et al.[40] Thus, the increased contribution of 6s electron polarization leads to a reduction of the effective hyperfine field. In the magnetically ordered state, the electric field gradient parameter used to optimize the fit changes by a factor about −0.2, indicating that the principal axis of the electric field gradient tensor is oriented to the direction of the magnetic hyperfine field with a polar angle of approximately 60°. At 78 K, a good fit of the magnetic hyperfine split spectrum is possible without a distribution of flux densities. However, disordering effects are also present and manifested by an increased line width.

The divalent europium hydride $EuRh_2H_x$[3] has a significantly lower isomer shift of $\delta = -10.82$ mm/s and this is indicative for much lower 6s electron density at the europium nuclei in $EuRh_2H_x$.

4. Conclusions

$EuRh_{1.2}Zn_{0.8}$ was synthesized in a high-frequency furnace and crystallizes as a pseudobinary cubic Laves phase, thus isotypic to $EuRh_2$. By the substitution of Rh by Zn we were able to reduce the Eu atoms from 3+ to 2+. Ferromagnetic ordering around 95 K was observed by magnetic measurements, which is to the best of our knowledge the highest ordering temperature, for a ternary intermetallic europium compound. ^{151}Mössbauer spectroscopic data are in line with the magnetic data. The dependence on the isomer shift vs VEC, described earlier,[15] is rounded up by the lowest negative isomer shift observed for $EuRh_{1.2}Zn_{0.8}$ corresponding to the lowest VEC.

We have also determined the MCE for $EuRh_{1.2}Zn_{0.8}$. Although the values of ΔS_M and ΔT_{ad} are significantly lower compared to those of giant MCE materials $EuRh_{1.2}Zn_{0.8}$ has a quite high normalized relative cooling power with 103 J K^{-1} T^{-1} for $\Delta H = 5$ T. This value is higher than that of previously investigated Laves phases in this temperature region.[41] This and the fact of lacking hysteresis loss makes $EuRh_{1.2}Zn_{0.8}$ an interesting cooling material. The experiences of our and previous works are showing the variety of tuning possibilities in europium-based Laves phases, concerning the magnetic properties and therefore MCE.

Acknowledgment. We are grateful to B. Heying and Dipl.-Ing. U. Ch. Rodewald for the intensity data collections. This work was supported by the Deutsche Forschungsgemeinschaft. W.H. is indebted to the Fonds der Chemischen Industrie for a PhD stipend. The doctoral thesis of T.H. is financed by the NRW Graduate School of Chemistry.

Supporting Information Available: Crystallographic data in CIF format. This material is available free of charge via Internet at http://pubs.acs.org.

(40) Wickman, H. H.; Nowik, I.; Wernick, J. H.; Shirley, D. A.; Frankel, R. B. *J. Appl. Phys.* **1966**, 37, 1246.
(41) Gorsse, S.; Chevalier, B.; Orveillon, G. *Appl. Phys. Lett.* **2008**, 92, 122501.